

A&A manuscript no.
(will be inserted by hand later)

Your thesaurus codes are:
11.03.1;11.04.1;11.05.02;11.06.2;11.09.2

The Richness-Shape Relation of the 2dFGRS Groups

M. Plionis^{1,2} and S. Basilakos¹

¹ Institute of Astronomy & Astrophysics, National Observatory of Athens, Palaia Penteli 152 36, Athens, Greece,

² Instituto Nacional de Astrofísica Óptica y Electrónica, AP 51 y 216, 72000, Puebla, Pue, México

Received ...2003 / Accepted .. 2003

Abstract. We estimate the group shape of the recently compiled Pecolation-Inferred Galaxy Group (2PIGG) catalogue. Using a set of integral equations we invert the projected distribution of group axial ratios and recover the corresponding intrinsic distribution under the assumption that groups are pure spheroids. In agreement with the analysis of the UZC-SSRS2 group sample (Plionis, Basilakos & Tovmassian 2004) we find that groups are extremely elongated prolate-like systems. We also find an interesting trend between shape and group richness with poorer groups being significantly flatter than richer ones.

Key words: galaxies: clusters: general – large-scale structure of Universe

1. Introduction

Groups of galaxies are the lowest level cosmic structures, after galaxies themselves, in the hierarchy that leads to the largest virialized structures, the clusters of galaxies. It appears that most galaxies are found in groups and they are therefore extremely important in our attempts to understand the cosmic structure formation processes. Since virialization will tend to sphericalize initial anisotropic distributions of matter, the shape of different cosmic structures is a possible indication of their evolutionary stage.

Theoretical and observational works have shown that the cosmic structures (clusters and superclusters) are dominated by prolate like shapes (cf. Carter & Metcalfe 1980; Plionis, Barrow & Frenk 1991; Cooray 1999; Basilakos, Plionis & Maddox 2000; Zeldovich, Einasto & Shandarin 1982; de Lapparent, Geller & Huchra 1991; Plionis, Jing & Valdarnini 1992; Jaaniste et al. 1998; Sathyaprakash et al. 1998; Valdarnini, Ghizzardi & Bonometto 1999; Basilakos, Plionis & Rowan-Robinson 2001). In the case of Groups of galaxies a recent study of the UGC-SSRS2 group catalogue (Plionis, Basilakos & Tovmassian 2004) have shown that they are extremely flat systems. Furthermore, their intrinsic shape appears to be that of a prolate-like spheroid (see also Oleak et al. 1995 and references therein).

In this letter we use the recently constructed 2PIGG group catalogue (Eke et al. 2004) which is based on the Two-Degree Field Galaxy Redshift Survey (2dFGRS) and contains 7020 groups with four or more galaxy members to estimate their projected and intrinsic shape as a function of their galaxy membership.

2. Sample and Shape Determination Method

The 2PIGG group catalogue (Eke et al. 2004) is constructed using a friends-of-friends (FOF) algorithm with linking parameters selected after thorough tests that have been applied on mock Λ CDM galaxy catalogues. The underline 2dFGRS catalogue used contain 191440 galaxies with well defined completeness limits for the survey geometry, the magnitude and redshift selection functions. The resulting 2PIGG group catalogue contains 7020 groups with at least 4 members having a median redshift of 0.11. Out of these 2975 and 4045 are found in the northern (NGP) and the southern (SGP) regions of the survey respectively.

The specific group finding algorithm used (Eke et al. 2004) treats in detail many issues that are related to completeness, the underlying galaxy selection function and the resulting biases that enter in attempts to construct unbiased group or cluster catalogues. In order to take into account the drop of the underlying galaxy number density with redshift, due to its magnitude limited nature, the authors have used a FOF linking parameter that scales with redshift. This scaling is variable also in the perpendicular and parallel to the line-of-sight direction with their ratio being ~ 11 (for details see the original paper of Eke et al. 2004). The necessity to increase the linking volume with redshift introduces biases in the morphological and dynamical characteristics of the resulting groups which should be taken into account before extracting any statistical information from the group catalogue. For example, an outcome of the above is the increase with redshift of both the velocity dispersion and the projected size of the candidate groups. In Fig.1 we present for the NGP and SGP samples with membership $n_m \geq 4$ their velocity dispersions and the mean projected member galaxy separa-

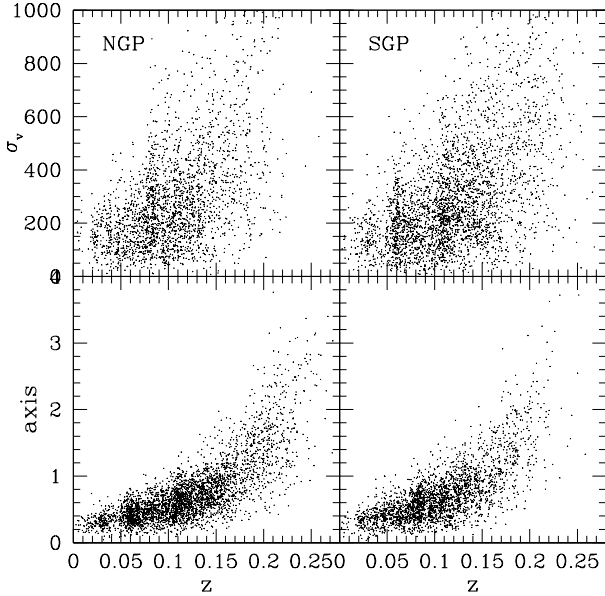


Fig. 1. The dependence of the group velocity dispersion (upper panels) and the mean member intergalaxy separation (lower panels) on redshift for the NGP and SGP samples.

tion. The redshift dependence is evident. Therefore, the probability that the groups found are real dynamical entities, should decrease with redshift. The best probably approach to deal with such systematics is the use of N-body simulations to test the effects of the algorithm and the parameters used as well as to calibrate the statistical results (Eke et al. 2004).

For our study of the shapes of the 2PIGG groups we will also follow some standard procedures to minimize possible systematics. To this end we extract group subsamples the number density of which, within some limiting redshift, is relatively constant, i.e., we select a roughly volume limited region. In Fig. 2 we show the group number density as a function of redshift in equal volume shells, which is roughly constant out to $cz \sim 30000 \text{ km s}^{-1}$. Within this limit we are left with 2980 groups with 4 or more members (1493 and 1487 in the NGP and SGP respectively).

2.1. Mean group shape parameters

We derive the projected group shape parameters using the moments of inertia method (cf. Carter & Metcalfe 1983; Basilakos et al. 2000). In Plionis et al. (2004) we performed a large number of Monte-Carlo simulations to test whether random projections could result in the observed distributions of axial ratios and we have excluded such possibility (without this meaning that some of the groups could not be contaminated by projections). Of course the probability of a group being false is inversely proportional to the group galaxy membership, n_m . Random projections will

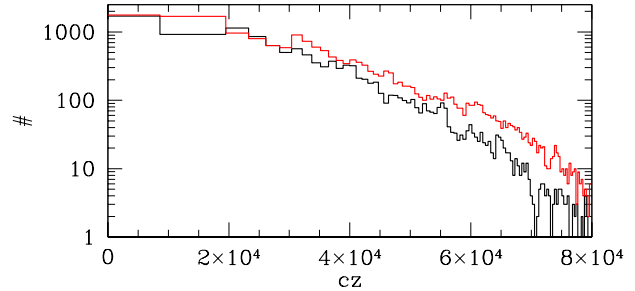


Fig. 2. The group number density in equal volume shells. The NGP/SGP subsample is represented by the lower/upper line.

Table 1. Summary of group subsample characteristics within $cz < 30000 \text{ km s}^{-1}$: N is the number of groups, $\langle z \rangle$ is their mean redshift, \bar{q} and \bar{a} are the median values of their axial ratios and member intergalaxy separation.

n_m	N	$\langle z \rangle$	\bar{q}	\bar{a}
NGP				
4	506	0.067	$0.31^{+0.09}_{-0.10}$	$0.41^{+0.09}_{-0.06}$
5-19	872	0.069	$0.42^{+0.08}_{-0.10}$	$0.56^{+0.12}_{-0.11}$
≥ 20	115	0.069	$0.56^{+0.08}_{-0.05}$	$1.17^{+0.27}_{-0.22}$
SGP				
4	493	0.066	$0.32^{+0.09}_{-0.10}$	$0.37^{+0.07}_{-0.05}$
5-19	897	0.065	$0.44^{+0.08}_{-0.09}$	$0.49^{+0.08}_{-0.08}$
≥ 20	97	0.061	$0.59^{+0.1}_{-0.06}$	$0.92^{+0.15}_{-0.11}$

affect significantly more the apparent characteristics (dynamical and morphological) of small groups rather than large ones and for this reason we have decided not to study groups with $n_m = 3$.

Based on their galaxy membership, n_m , we will study separately groups with $n_m = 4$, $4 \leq n_m < 20$ and $n_m \geq 20$, the latter being nearer to the definition of a cluster.

The summary of the main structure parameters of the different membership samples of groups is presented in Table 1. The first and second columns give the group membership and the number of such groups respectively, the third column gives their mean redshift while the fourth and fifth columns show the median values of the projected axial ratio (\bar{q}) and intergalaxy separation (\bar{a}), together with their 68% and 32% quantile values. It is evident that the considered groups are very elongated, significantly more than what expected from random projections of field galaxies (see Plionis et al. 2004), giving support to them being real dynamical entities.

A certain correlation is apparent between \bar{q} and \bar{a} increasing with n_m . We find that the mean redshift of each group subsample is constant and thus the increase of the group size with n_m cannot be due to the increase with

redshift of the group linking volume which induces the systematic trend seen in Fig.1.

The increase of the group sphericity with n_m could be explained as an indication of a higher degree of virialization, which is expected to be more rapid in systems containing more galaxies (mass). Virialization processes increase the sphericity of systems but also compactifies them from their original dispersed configuration, assuming that they accrete mass anisotropically along large-scale filaments (cf. West 1994). The increase with n_m of the group sizes, which is also accompanied with a decrease of the galaxy density, dropping from ~ 160 to $\sim 20 h^3 \text{ Mpc}^{-3}$ for the $n_m = 4$ and $n_m \geq 20$ groups respectively (assuming a prolate group shape- see next session), is quite intriguing.

Finally, comparing the 2PIGG shape parameters with those of the UGC-SSRS2 groups (Plionis et al. 2004) we find quite similar results. For example, the median q of the $4 \leq n_m \leq 10$ groups are $\sim 0.33 \pm 0.09$ and $\sim 0.36 \pm 0.09$ for the UGC-SSRS2 and 2PIGG samples, respectively.

2.2. The projected axial ratio distribution

The derived discrete frequency distribution of the projected group axial ratio is fitted by a continuous function using the so-called kernel estimators (for details see Ryden 1996 and references therein) Although we will not review this method we note that the basic kernel estimate of the frequency distribution is defined as:

$$\hat{f}(q) = \frac{1}{Nh} \sum_i^N K\left(\frac{q - q_i}{h}\right), \quad (1)$$

where q_i are the group axial ratios and $K(t)$ is the kernel function (assumed here to be a Gaussian), defined so that $\int K(t)dt = 1$, and h is the ‘‘kernel width’’ which determines the balance between smoothing and noise in the estimated distribution. The value of h is chosen so that the expected value of the integrated mean square error between the true, $f(q)$, and estimated, $\hat{f}(q)$, distributions is minimised (cf. Vio et al. 1994; Tremblay & Merritt 1995).

In Figure 3 we present the projected axial ratio distributions for the different membership groups (circles), as indicated in the different panels, with their Poisson 1σ error bars, while the solid lines shows the kernel estimate \hat{f} for the appropriate width, h . As the membership number increases, there is evidently a shift to less flattened systems, with the peak of the axial ratio distribution shifting from $q \simeq 0.22$ to ~ 0.4 and ~ 0.55 for groups with $n_m = 4$, $5 \leq n_m < 20$ and $n_m \geq 20$, respectively.

2.3. True Group Shapes

As in Plionis et al. (2004) we invert the projected axial ratio distribution assuming that groups are either oblate or prolate spheroids. Although there is no physical justification for this restriction, it greatly simplifies the inversion

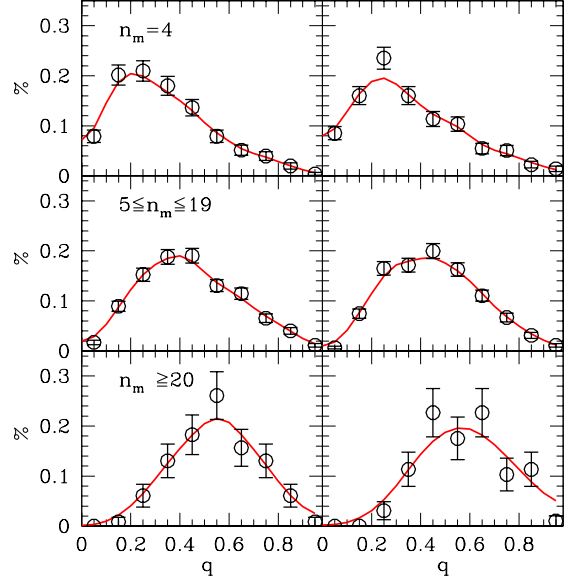


Fig. 3. The apparent axial ratio distributions for different group membership. The solid line is the smooth fit from the nonparametric kernel estimator. LEFT PANEL: The NGP subsample, RIGHT PANEL: The SGP subsample.

problem. Furthermore, if groups are a mixture of the two spheroidal populations or they have triaxial configurations then there is no unique inversion (Plionis et al. 1991).

Under the above restriction and the assumption that the orientation of groups is random with respect to the line of sight, the relation between the apparent and intrinsic axial ratios can be described by a set of integral equations, first investigated by Hubble (1926). Writing the intrinsic axial ratios as β and the estimated distribution function as $\hat{N}_o(\beta)$ for oblate spheroids, and $\hat{N}_p(\beta)$ for prolate spheroids then the corresponding distribution of apparent axial ratios is given for the oblate case by:

$$\hat{f}(q) = q \int_0^q \frac{\hat{N}_o(\beta) d\beta}{(1 - q^2)^{1/2} (q^2 - \beta^2)^{1/2}} \quad (2)$$

and for the prolate case by:

$$\hat{f}(q) = \frac{1}{q^2} \int_0^q \frac{\beta^2 \hat{N}_p(\beta) d\beta}{(1 - q^2)^{1/2} (q^2 - \beta^2)^{1/2}}. \quad (3)$$

Inverting equations (eq.2) and (eq.3) gives us the distribution of real axial ratios as a function of the measured distribution:

$$\hat{N}_o(\beta) = \frac{2\beta(1 - \beta^2)^{1/2}}{\pi} \int_0^\beta \frac{d}{dq} \left(\frac{\hat{f}}{q} \right) \frac{dq}{(\beta^2 - q^2)^{1/2}} \quad (4)$$

and

$$\hat{N}_p(\beta) = \frac{2(1 - \beta^2)^{1/2}}{\pi\beta} \int_0^\beta \frac{d}{dq} (q^2 \hat{f}) \frac{dq}{(\beta^2 - q^2)^{1/2}}. \quad (5)$$

with $\hat{f}(0) = 0$. The important point here is that in order for $\hat{N}_p(\beta)$ and $\hat{N}_o(\beta)$ to be physically meaningful they should be positive for all β 's. Negative values indicate that the model is unacceptable. Integrating numerically eq.(4)

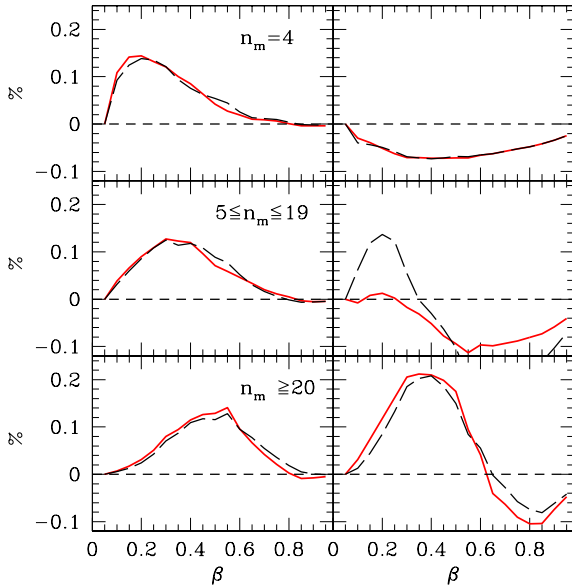


Fig. 4. The distribution of the intrinsic 2dFGRS group axial ratios for the NGP (continuous line) and SGP (dashed line) subsamples assuming that they are either prolate (left panel) or oblate (right panel) spheroids.

and eq.(5) allowing $\hat{N}_p(\beta)$ and $\hat{N}_o(\beta)$ to take any value, we derive the inverted (3D) axial ratio distributions, which we present in Figure 4.

The oblate model is completely unacceptable since it produces negative values of the inverted intrinsic axial ratio distribution. Therefore, we can conclude that the 2PIGG groups shape is well represented only by that of prolate spheroids which is in agreement with the previous analysis of the UGC-SSRS2 poor groups (Plionis et al. 2004) and Shakhbazian compact groups (Oleak et al. 1995).

The richer groups ($n_m \geq 20$) have an intrinsic axial ratio distribution that approximates that of clusters of galaxies, as can be seen in Fig. 5 where we compare with the APM cluster shapes for the prolate case (which is also the best spheroidal model for clusters; see Plionis et al. 1991, Basilakos et al. 2000).

3. Conclusions

We have measured the projected axial ratio distribution of the 2PIGG groups of galaxies within a roughly volume-limited region ($cz \leq 30000$ km/sec). Assuming that groups constitute a homogeneous spheroidal population, we numerically invert the projected axial ratio distribution to obtain the corresponding intrinsic one. The only acceptable model is that of prolate spheroids which is in excellent agreement with the analysis of the UGC-SSRS2 sample of poor groups (Plionis et al. 2004).

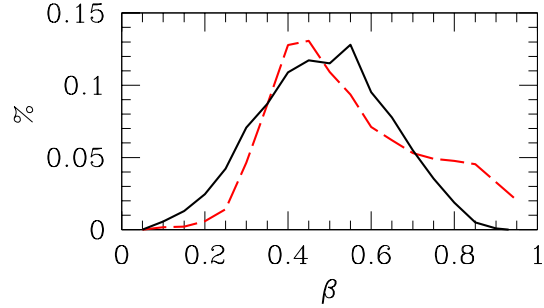


Fig. 5. Comparison of the intrinsic ($n_m \geq 20$) group axial ratio distribution (continuous line) with that of the APM cluster (dashed line; from Basilakos et al. 2000) for the prolate model.

There is an obvious group richness-flatness relation, seen in both projected and intrinsic axial ratio distributions, with poorer groups being also the flatter. For example, the peak of the projected axial ratio distribution shifts from $q \sim 0.22$ for groups with only 4 members to ~ 0.55 for those with more than 19 members. The increase of the group sphericity with richness, which extends also to clusters, could be explained as an indication of a higher degree of virialization, which is expected to be more rapid in more massive systems.

Acknowledgments

This research was jointly funded by the European Union and the Greek Government within the program 'Promotion of Excellence in Technological Development and Research'. MP also acknowledges funding by the Mexican Government grant No. CONACyT-2002-C01-39679.

References

- Basilakos, S., Plionis, M., Maddox, S.J., 2000, MNRAS, 316, 779
- Basilakos, S., Plionis, M., Rowan-Robinson, M., 2001, MNRAS, 323, 47
- Carter, D. & Metcalfe, J., 1980, MNRAS, 191, 325
- Cooray, R.A., 2000, MNRAS, 313, 783
- de Lapparent, V., Geller, M.J., Huchra, J.P., 1991, ApJ, 369, 273
- Eke, V.K., et al., 2004, MNRAS, 348, 866
- Jaaniste, J., Tago, E., Einsato, M., Einsato, J., Andernach, H., Mueller, V., 1998, A&A, 336, 35
- Oleak H., Stoll D., Tiersch H., MacGillivray H.T. 1995, AJ, 109, 1485
- Plionis M., Barrow J.D., Frenk, C.S., 1991, MNRAS, 249, 662
- Plionis M., Valdarnini, R., Jing, Y.P. 1992, ApJ, 398, 12
- Plionis, M., Basilakos, S. & Tovmassian, H., 2004, MNRAS, *submitted*, astro-ph/0312019
- Ryden S.B., 1996, ApJ, 461, 146
- Sathyaprakash, B.S., Sahni, V., Shandarin, S.; Fisher, K.B., 1998, ApJ, 507, L109

- Tremblay, B., & Merrit, D., 1995, *AJ*, 110, 1039
Valdarnini, R., Ghizzardi, S., Bonometto, S., 1999, *NewA*, 4,
71
Vio, R., Fasano, G., Lazzarin, M., Lessi, O., 1994, *AA*, 289,
640
West, M.J., 1994, *MNRAS*, 268, 79
Zeldovich, Ya. B., Einasto, J., Shandarin, S., 1982, *Nature*, 300,
407